



RESEARCH ARTICLE

Open Access



The Potential of *Murraya koenigii* as a PfAp4AH Inhibitor for Malaria Drug Development

Inda Setyawati^{1,*}, Assifah Eryandini¹, Nadine Rudiyana¹, Laksmi Ambarsari¹, I Made Artika¹

Abstract

Murraya koenigii, a medicinal plant from the Rutaceae family, is traditionally used as a flavoring agent and is known for its bioactive carbazole alkaloids. Native to the Indo-Malaysian region, China, Sri Lanka, and New Caledonia, this plant has shown potential for therapeutic applications, including antimalarial activity. Malaria, particularly caused by *Plasmodium falciparum*, remains a significant global health challenge due to rising drug resistance. PfAp4AH, an enzyme involved in diadenosine tetraphosphate (Ap4A) metabolism, has emerged as a promising target for novel antimalarial drugs.

This study employed computational approaches—binding site prediction and virtual screening through molecular docking—to identify potential PfAp4AH inhibitors from 156 carbazole alkaloids derived from *M. koenigii*. Ten compounds demonstrated stronger binding affinities than ATP, with compound 1 showing the highest inhibitory potential through strong and diverse interactions with key residues Tyr87, His43, Pro133, and Leu136. These findings underscore the importance of specific ligand-residue interactions in determining binding strength. The identified compounds, especially compound 1, present promising leads for further experimental validation. While initial bioactivity and toxicity profiles are favorable, comprehensive bioavailability and toxicological evaluations are needed to advance these compounds as antimalarial drug candidates.

Keywords: Antimalarial, Carbazole Alkaloids, Molecular Docking, *Murraya koenigii*, PfAp4AH

1. Introduction

Murraya koenigii is a medicinal plant used in traditional Indian medicine, such as the Ayurveda and Siddha systems. The cultivation has extended to Reunion island, Yunnan, Laos, Pakistan, Sri Lanka, Nepal, Malaysia, South Africa, Bhutan, Thailand, Indonesia, Myanmar, southern China, Hainan, Pacific islands, Australia, South Texas, South Florida and Southern California (Suthar et al., 2022). The leaves, bark and root of this plant have been extensively studied for its diverse bioactive compounds, especially carbazole alkaloids, known for their pharmacological potential, including antimicrobial, antidiabetic, and anticancer activities (Patel et al., 2016a; Uvarani et al., 2013). Considering these properties, compounds derived from *M. koenigii* represent an attractive source of potential PfAp4AH inhibitors.

Malaria remains one of the most significant public health challenges worldwide, causing hundreds of

thousands of deaths annually, primarily in tropical and subtropical regions (World Health Organization (WHO), 2022). *Plasmodium falciparum* is responsible for the majority of severe malaria cases and exhibits increasing resistance to existing antimalarial therapies, underscoring the urgent need for novel therapeutic targets and new drug candidates (Ashley et al., 2018; White et al., 2014).

Among emerging therapeutic targets, diadenosine tetraphosphate hydrolase from *P. falciparum* (PfAp4AH) has attracted attention due to its critical role in parasite metabolism. PfAp4AH catalyzes the hydrolysis of diadenosine tetraphosphate (Ap4A), a molecule involved in cellular processes such as stress responses, energy metabolism, and signal transduction (Ali et al., 2021; Sharma et al., 2016a). Given its essential function, inhibition of PfAp4AH represents a promising and innovative strategy to control *Plasmodium* proliferation.

However, the absence of crystal structures of

*Correspondence: inda_setyawati@apps.ipb.ac.id

1) Institut Pertanian Bogor - Jl. Raya Dramaga, Kampus IPB Dramaga, Bogor 16680 West Java, Indonesia

PfAp4AH complexed with known inhibitors complicates the rational design of targeted therapeutics. As a result, computational methods such as virtual screening and molecular docking have become essential for predicting potential inhibitors and exploring their interactions with the active site of PfAp4AH (Ali et al., 2021).

This study utilized computational approaches, including binding site prediction and virtual screening through molecular docking, to identify promising carbazole alkaloids from *M. koenigii* as novel PfAp4AH inhibitors. Previous studies have explored PfAp4AH as a therapeutic target using synthetic compounds or broad ligand libraries (Ali et al., 2021), but investigations focusing specifically on natural carbazole alkaloids from *M. koenigii* remain limited. Unlike earlier works, this study emphasizes structure-based screening of phytochemicals derived from a single medicinal plant known for its antimalarial properties. By evaluating the binding interactions and affinities of these compounds with critical residues in the PfAp4AH active site, this research highlights a new natural source of potential inhibitors and offers mechanistic insights that can guide future experimental validation and antimalarial drug development.

2. Material and Methods

The experiment was conducted between December 2021 and February 2023 at the Biochemistry Laboratory, IPB University, Bogor, Indonesia. 6.55699° S, 106.72527° E, at an altitude of 188 meters (masl). An overview of the research methodology is illustrated in the research flowchart (Figure 1).

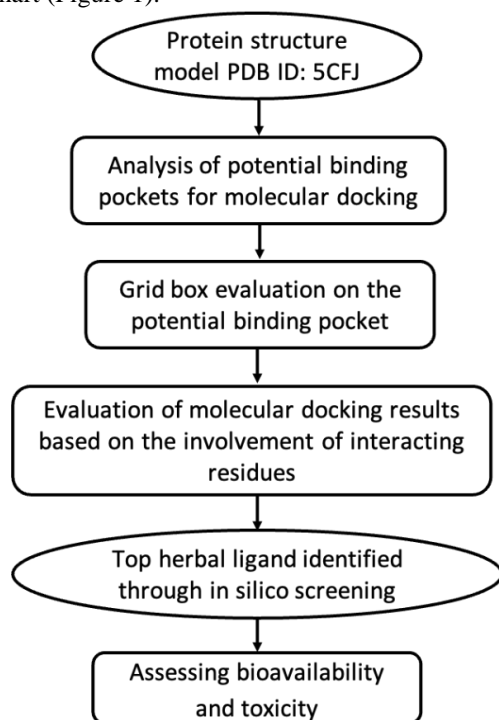


Figure 1. The flowchart of research methodology

2.1. Binding Pocket Analysis for Docking Target

The binding pocket of the PfAp4AH target protein, intended for candidate drug molecules, was identified using the PockDrug server (modified from (Ali et al., 2021)). On the PockDrug website, the "Druggability Prediction" menu was selected, and the target protein's PDB code (PDB ID: 5CFJ) was entered. Pocket estimation was conducted using the fpocket parameter with a ligand proximity threshold set at 5.5 Å .

2.2. Identification of Conserved Amino Acid Residues in the Binding Pocket

Sequence analysis for conserved amino acid residues within the PfAp4AH binding pocket was performed using the ConSurf server (<https://consurf.tau.ac.il>) (Ashkenazy et al., 2016). The conserved amino acids were analyzed by entering the protein's PDB code into the ConSurf website. Default parameters for homology algorithms were selected, and homolog analysis was conducted automatically by selecting "automatically." The sequence analysis was set to "closest to reference sequence," utilizing Bayesian calculations. The analysis was then submitted for processing. The resulting output was a protein structure in PDB format with a *.py script. The potential druggable pocket identified from druggability analysis was visualized using PyMol by loading the ConSurf-generated *.py script. The pocket visualization used a color scale to indicate the conservation level of each amino acid residue.

2.3. Preparation of Receptor and Ligand Structures

The 3D structural models of Ap4AH from *Aquifex aeolicus* (AaAp4H, 3I7V (Jeyakanthan et al., 2010) and PfAp4AH (5CFJ, (Sharma et al., 2016b) were obtained from the RCSB Protein Data Bank (<https://www.rcsb.org/>) in ".pdb" format. AaAp4H has been crystallographically elucidated with ATP bound at its active site, enabling the prediction of ATP binding poses in PfAp4AH, following methods previously described by (Ali et al., 2021). The ATP binding pose in PfAp4AH was estimated by superimposing (aligning) structures 3I7V and 5CFJ using PyMol software, resulting in a protein structure file in ".py" format.

Ligand structures were retrieved from the HerbalDB database and PubChem (<https://pubchem.ncbi.nlm.nih.gov/>) and downloaded in ".sdf" format. Complete ligand information and structural data were previously (Setyawati, Ilyas, et al., 2024; Setyawati, Setiawan, et al., 2024). Subsequently, OpenBabel software was utilized to reduce the ligands and convert their structures from ".sdf" to ".pdbqt" format, making them compatible for molecular docking procedures. The ligand data were then compiled into a single compressed folder in ".zip" format (modified previously (Setyawati, Ilyas, et al., 2024; Setyawati, Setiawan, et al., 2024).

2.4. Validation of Molecular Docking

Validation of molecular docking was conducted using Google Colab Pro and Autodock Tools. The validation involved docking the ATP ligand, originally co-crystallized with AaAp4AH (PDB ID: 3I7V). The ATP ligand was validated by docking it into the active site occupied by the co-crystallized ATP in AaAp4AH to predict its docking site in PfAp4AH and AaAp4H. This approach was facilitated by the superimposition of AaAp4AH (3I7V) and PfAp4AH (5CFJ) using PyMol software (DeLano Scientific, Palo Alto, CA, USA). The results showed that the adenosine ring of ATP resides in a pocket formed by residues Tyr87, Pro133, and Ser135.

The three-dimensional structures of the receptor and ligand were saved in PDBQT format. Before docking, the protein was prepared using Autodock Tools by removing water molecules, adding hydrogen atoms, and eliminating unnecessary residues. The receptor in PDBQT format was then opened, and grid box dimensions were set using size parameters (size x, y, z) and center parameters (center x, y, z). Docking outcomes provided values for binding affinity and RMSD for each predicted pose. More negative RMSD values indicated higher docking accuracy.

2.5. Virtual Screening by Molecular Docking

The virtual screening process began by opening the receptor and test ligand files in Google Colab Pro to define the grid box size. Input parameters in Google Colab Pro included receptor name, ligand name, grid box dimensions, and exhaustiveness (set up to 20 Å). The grid box defines the 3D area surrounding the target protein where the docking algorithm searches for optimal ligand binding poses. Subsequently, the processed receptor protein was validated by optimizing the grid box extension to achieve optimal free energy and an RMSD value below 2 Å. Validation was performed over 10 runs.

The second virtual screening approach utilized AutoDock-GPU. Prepared receptor and ligand files had their grid box dimensions set by targeting the three amino acid residues Tyr87, Pro133, and Ser135 within the PfAp4AH receptor. Validation results were saved in PDB format for use in virtual screening. All test ligand compounds in PDBQT format were consolidated into a single *.zip folder, and then uploaded into Google Colab Pro along with the receptor file and grid box coordinates. Virtual screening commenced upon clicking "RUN," producing ligand files in PDBQT format, log files containing binding affinity values (kcal/mol) and RMSD (root-mean-square deviation), and ligand docking poses on the receptor. The ligand pose exhibiting the most negative optimal Gibbs free energy (ΔG) value was selected.

Discovery Studio (BIOVIA) and PyMOL software were employed to create three-dimensional visual representations of interactions between test ligands and amino acid residues within the protein. Three-dimensional

visualization of virtual screening and molecular docking results was performed by aligning ligand poses using PyMOL. Receptor and ligand files in PDBQT format were loaded into PyMOL, where alignment was utilized to accurately position predicted ligand binding poses relative to the target protein structure. The receptor was depicted using a surface representation with 20% transparency. Residues interacting with ligands were illustrated as sticks in contrasting colors and labeled clearly. Ligands identified from the virtual screening were visualized to compare their respective binding poses. Visualization of ligand-residue interactions was carried out using Discovery Studio software, providing both two-dimensional and three-dimensional interaction representations.

2.6. Assessing Bioavailability and Toxicity

The bioavailability and toxicity profiles of dimeric carbazole alkaloids (compounds 1–10) were assessed through a literature-based study. Relevant scientific articles, reviews, and pharmacological databases were systematically searched using keywords such as "*Murraya koenigii*," "dimeric carbazole alkaloid," "bioavailability," "toxicity," "safety," and specific compound names (e.g., yuehchukene, chrestifoline A). Primary data were extracted from peer-reviewed sources that reported experimental or observational findings on the biological activity, pharmacokinetics, and toxicity of these compounds or their plant extracts. The compiled information provided insight into general safety trends, while highlighting the limited availability of detailed, compound-specific bioavailability and toxicity evaluations.

3. Results and Discussion

3.1. Potential Docking Sites

To identify potential docking sites, a combination of druggability analysis and residue conservation assessment in amino acid pockets was conducted. This analysis aimed to determine the active site of *P. falciparum* diadenosine tetraphosphate hydrolase (PfAp4AH), for which no ligand-bound structural data is currently available. The apo state model (PDB: 5CFJ) was used as a structural model, and the PockDrug server was employed to identify the characteristics of pockets suitable as drug-binding sites.

From the analysis, two pockets were identified in PfAp4AH: Pocket 1 (P1) and Pocket 2 (P2) (Figure 2A). The P1 has a druggability score of 0.31 (Table 1), while the P2 has 0.01. P1 shows potential as a docking site for virtual screening due to its larger volume (726 Å³) and higher druggability score compared to P2. Figure 2B and 2C illustrate the conservation levels of amino acid residues in P1 and P2, respectively. The visualization indicates that P2 contains more conserved residues, while P1 displays greater variability in residue conservation.

To further refine the docking site selection, the presence of amino acid residues unique to PfAp4AH, but

absent in human Ap4AH (HsAp4AH), was considered. Based on prior structural alignment (Sharma et al., 2016), P133 and S135, located in P1, were identified as unique residues (Figure 3A). Despite P1 having lower conservation compared to P2, these residues are expected to allow drug candidates to interact specifically with PfAp4AH while avoiding affinity for HsAp4AH.

Structural comparison studies by (Sharma et al., 2016b) revealed that human and *P. falciparum* Ap4AHs

exhibit differences in substrate-binding pockets. Notably, in human Ap4AH, Phe128 stacks with the adenine ring of the substrate, and E130 forms a hydrogen bond with the amino group of the adenine. These residues are replaced by smaller residues, P133 (for Phe128) and Ser135 (for E130), in PfAp4AH. These key differences create space for structural mimics of ATP or Ap4A to specifically target PfAp4AH, providing an opportunity for the design of selective inhibitors.

Table 1. Pocket analysis results for PfAp4AH

Pocket	Volume Hull (Å ³)	Kyte Hydrophobicity	Polar Residues	Aromatic Residues	Druggability Score	Standard Deviation
P1	725.96	-1.25	0.75	0.19	0.31	0.18
P2	431.12	-2.44	0.9	0.1	0.01	0.0

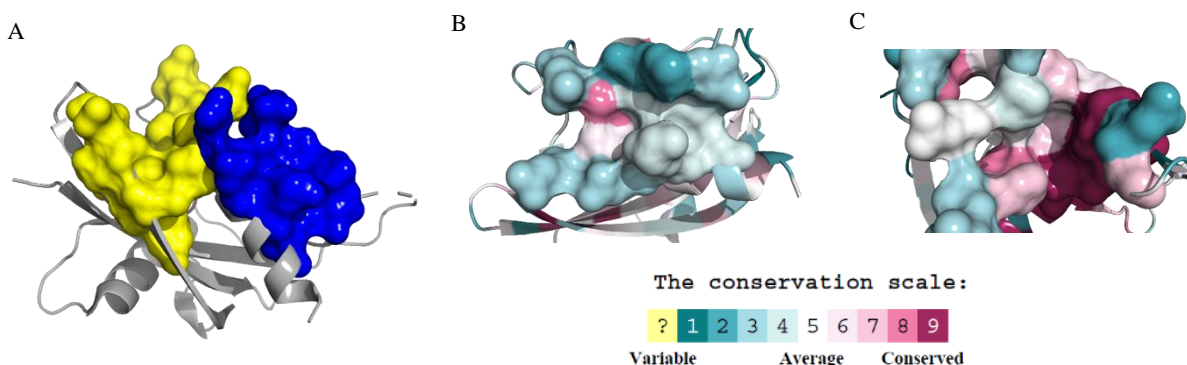


Figure 2. Druggability Pockets in PfAp4AH: A. Surface representation showing P1 (yellow) and P2 (blue); B. Conservation levels of residues in P1; C. Conservation levels of residues in P2.

Molecular Docking Validation with ATP as Ligand

Adenosine triphosphate (ATP) is a known ligand for Ap4AH, but this has only been experimentally confirmed for *Aquifex aeolicus* Ap4AH (AaAp4AH) and not for *P. falciparum* Ap4AH (PfAp4AH). To validate the docking algorithm used for virtual screening, the ATP pose from structural alignment between receptor models 5CFJ (apo PfAp4AH) and 3I7V (ATP-bound AaAp4AH) was compared with the ATP pose obtained through molecular docking at P1 (Figure 2A). The docking approach aimed to position ATP so its adenine group could interact with the three substrate-binding residues (Tyr87, Pro133, and Ser135) identified in the 3I7V structure (Sharma et al., 2016b).

The structural alignment using this three-residue approach evaluated whether docking could correctly position ATP near Tyr87, Pro133, and Ser135, supporting its use in virtual screening for PfAp4AH ligand candidates. The docking grid box, determined using AutoDock4, had dimensions of 20×20×20 Å³ with a spacing of 0.375 Å. This approach yielded a root mean square deviation (RMSD) of 2.408 Å and a binding affinity of -6.3 kcal/mol.

The ATP ligand pose alignment was performed using PyMOL, while the PfAp4AH protein data from RCSB PDB

was used to visualize the active site. Figure 3 illustrates that the docked ATP ligand interacts with Pro133 but not with Tyr87 and Ser135. Seven residues are depicted as sticks to highlight the interactions between ATP and PfAp4AH (Figure 3B). Two ligand poses are shown: the magenta ligand represents the ATP pose from structural alignment between models 5CFJ and 3I7V, while the orange ligand is the ATP pose from AutoDock4 re-docking (Figure 3A).

The alignment in Figure 2A demonstrates that the re-docked ATP ligand closely matches the superimposed ligand pose, validating the docking method's ability to reproduce critical interactions and orientations of ATP in the binding site. A 2D visualization of ATP's interactions with the PfAp4AH receptor (PDB: 5CFJ) was generated using Discovery Studio (Figure 3B). Key residues, including His43, His116, Lys94, Lys98, Pro133, and Thr45, interact with ATP through various non-covalent bonds, as shown in Figure 3B. This molecular docking validation confirmed the reliability of the docking protocol by accurately positioning ATP within the PfAp4AH active site. This validation supports the use of this approach for the identification of potential inhibitors through virtual screening.

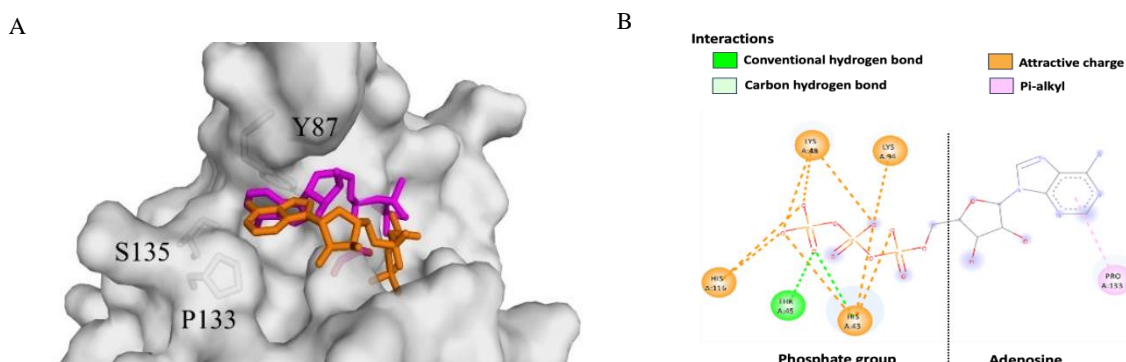


Figure 3. Predicted ATP Poses on PfAp4AH pocket (P1): A. The ATP pose obtained through molecular docking (orange) compared with the ATP pose (magenta) aligned between the receptor models 5CFJ (surface) and 3I7V; B. Visualization of ATP ligand interactions from the molecular docking results.

3.2. Carbazole Compounds Identified by Virtual Screening as Potential PfAp4AH Inhibitors

Virtual screening targeted a specific binding pocket in PfAp4AH, defined by residues Tyr87, Pro133, and Ser135, based on predictions from ATP docking studies. A total of 156 compounds derived from the curry leaf tree (*M. koenigii*) were screened and ranked by their predicted Gibbs free energy (ΔG) from docking simulations performed using Autodock4.

From this screening, the top ten compounds were identified with promising binding affinities as potential PfAp4AH inhibitors (Table 2), demonstrating higher binding affinities compared to ATP. The selected compounds include 1-(2-hydroxy-3-methyl-9H-carbazol-1-yl)-3-methyl-9H-carbazol-2-ol (compound 1), bismurrayaquinone A (compound 2), yuehchukene

(compound 3), (3R)-10-[(3R)-9-hydroxy-3,5-dimethyl-3-(4-methylpent-3-enyl)-11H-pyrano[3,2-a]carbazol-8-yl]-3,8-dimethyl-3-(4-methylpent-3-enyl)-11H-pyrano[3,2-a]carbazol-9-ol (compound 4), chrestifoline A (compound 5), bikoenuquinone A (compound 6), 8,8'-biskoenuigine (compound 7), (3R)-10-[(3R)-9-hydroxy-3,5-dimethyl-3-(4-methylpent-3-enyl)-11H-pyrano[3,2-a]carbazol-8-yl]-3,5-dimethyl-3-(4-methylpent-3-enyl)-11H-pyrano[3,2-a]carbazol-9-ol (compound 8), (3R)-10-[(3R)-8-hydroxy-3,5-dimethyl-3-(4-methylpent-3-enyl)-11H-pyrano[3,2-a]carbazol-10-yl]-3,5-dimethyl-3-(4-methylpent-3-enyl)-11H-pyrano[3,2-a]carbazol-9-ol (compound 9), and 3,3'-[Oxybis(methylene)]bis(9-methoxy-9H-carbazole) (compound 10).

Table 2. Top ten ligands from virtual screening of *M. koenigii* compounds

No.	Ligands	ΔG Docking (kcal/mol)
1	1-(2-hydroxy-3-methyl-9H-carbazol-1-yl)-3-methyl-9H-carbazol-2-ol	-8.0
2	Bismurrayaquinone A	-7.7
3	Yuehchukene	-7.5
4	(3R)-10-[(3R)-9-hydroxy-3,5-dimethyl-3-(4-methylpent-3-enyl)-11H-pyrano[3,2-a]carbazol-8-yl]-3,8-dimethyl-3-(4-methylpent-3-enyl)-11H-pyrano[3,2-a]carbazol-9-ol	-7.4
5	Chrestifoline A	-7.3
6	Bikoenuquinone A	-7.3
7	8,8'-Biskoenuigine	-7.2
8	(3R)-10-[(3R)-9-hydroxy-3,5-dimethyl-3-(4-methylpent-3-enyl)-11H-pyrano[3,2-a]carbazol-8-yl]-3,5-dimethyl-3-(4-methylpent-3-enyl)-11H-pyrano[3,2-a]carbazol-9-ol	-7.2
9	(3R)-10-[(3R)-8-hydroxy-3,5-dimethyl-3-(4-methylpent-3-enyl)-11H-pyrano[3,2-a]carbazol-10-yl]-3,5-dimethyl-3-(4-methylpent-3-enyl)-11H-pyrano[3,2-a]carbazol-9-ol	-7.2
10	3,3'-[Oxybis(methylene)]bis(9-methoxy-9h-carbazole)	-7.0

As detailed in Table 3, the carbazole compounds interacted distinctly with specific amino acid residues within the PfAp4AH active site, particularly the catalytic residues Tyr87, Ser135, and Pro133. Six compounds—1, 2, 3, 5, 6, and 10—interacted with both Tyr87 and Pro133, highlighting their importance. At least four compounds specifically interacted with Pro133, underscoring its crucial role in ligand stabilization within PfAp4AH.

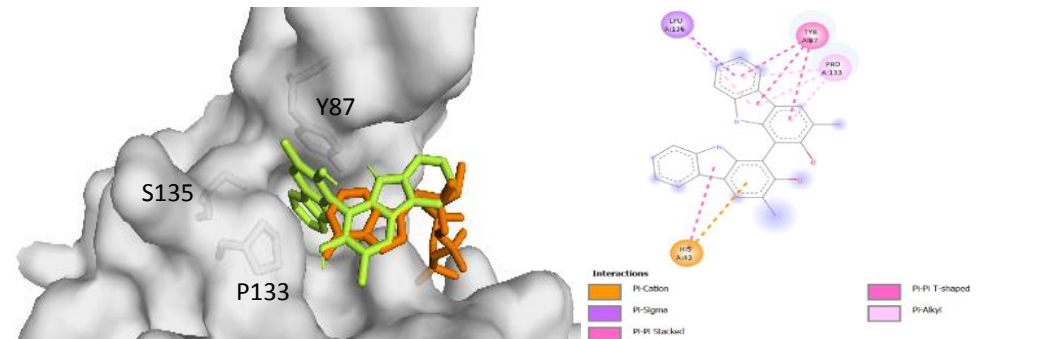
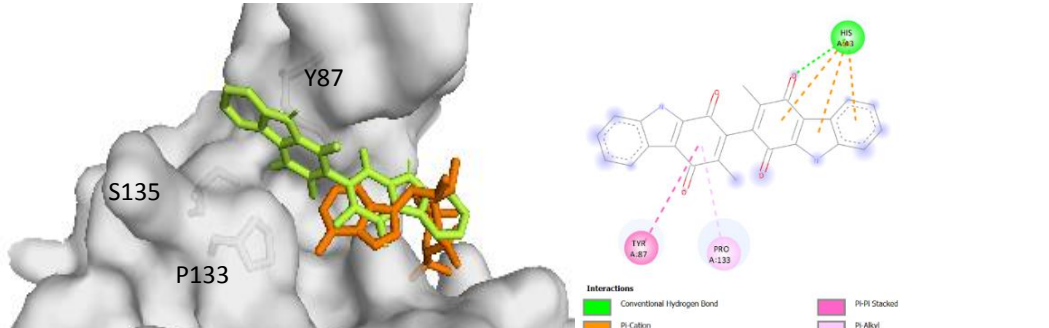
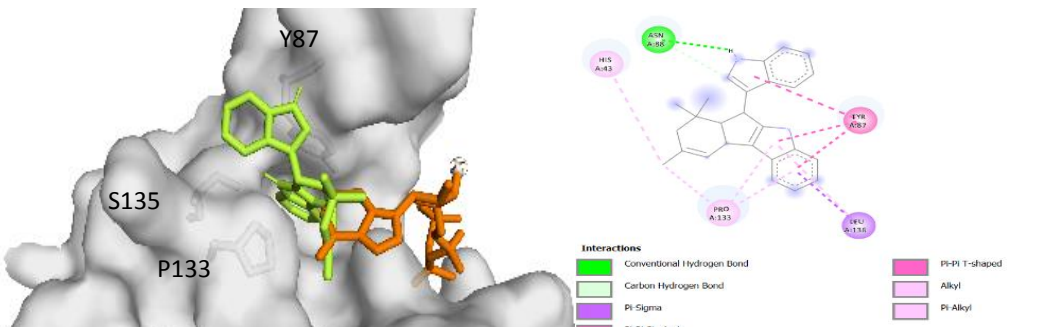
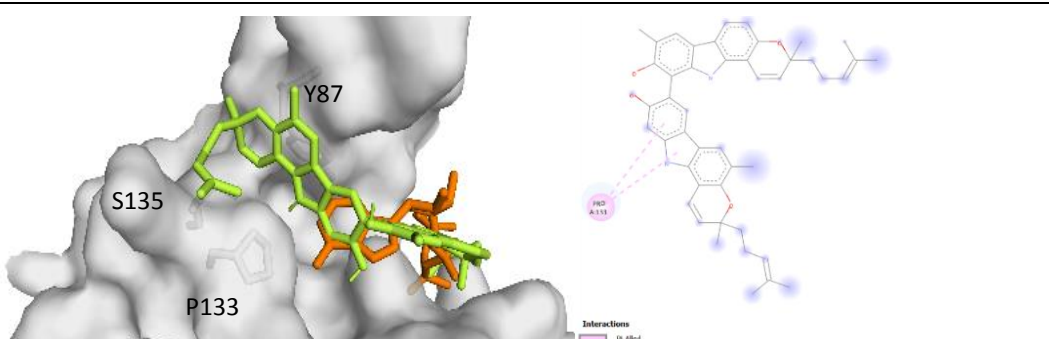
All ten carbazole candidates demonstrated pi-alkyl interactions with Pro133, while six compounds exhibited pi-pi stacking interactions with Tyr87. Compound 1 was identified as the most potent inhibitor, interacting with four key residues—Tyr87, His43, Pro133, and Leu136—through various bond types, including pi-cation (His43), pi-sigma (Leu136), pi-pi stacked and pi-pi T-shaped (Tyr87), and pi-alkyl (Pro133), significantly enhancing its stability

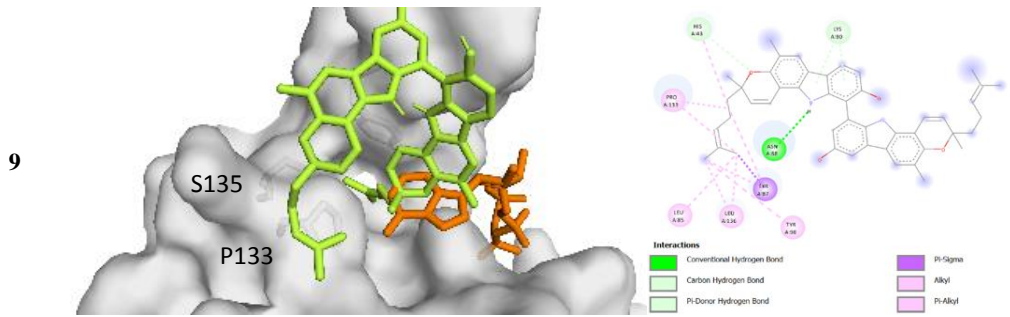
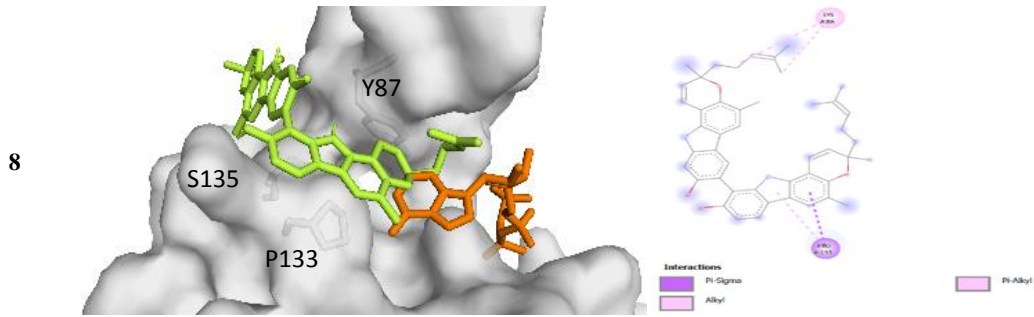
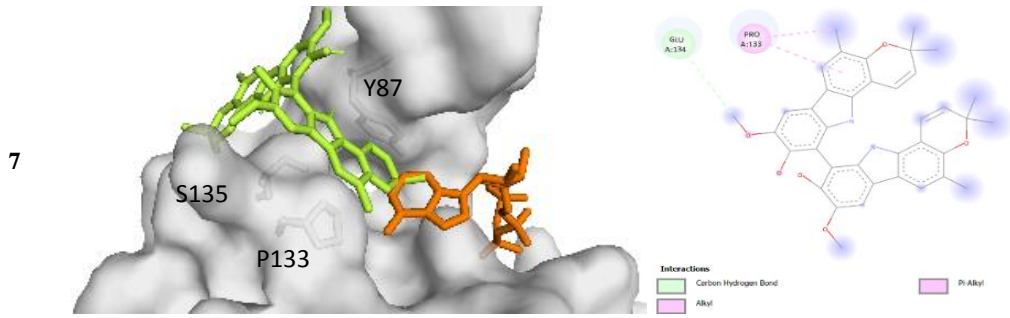
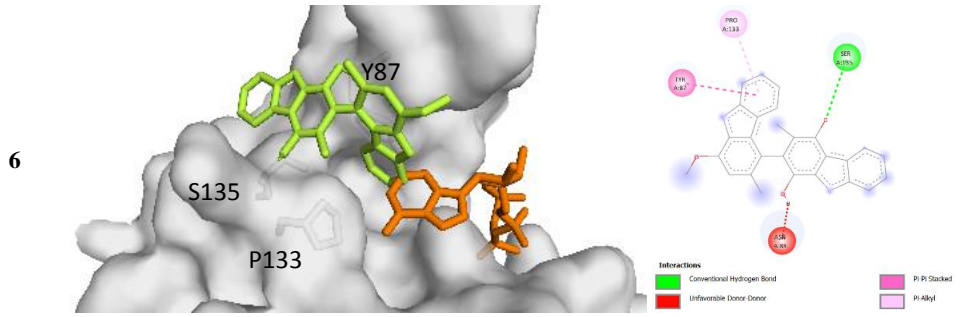
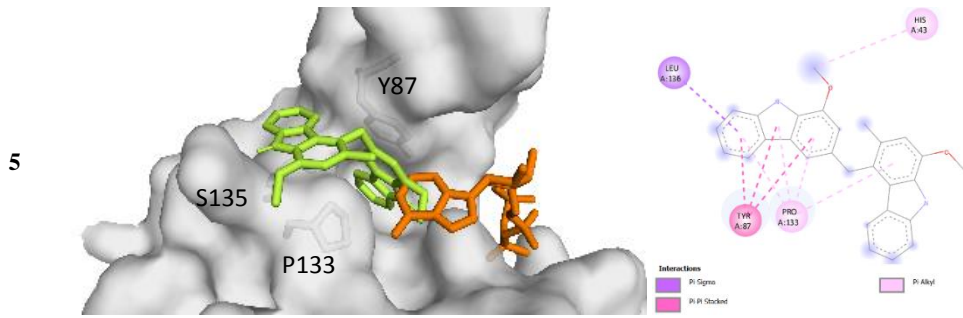
and inhibitory potential.

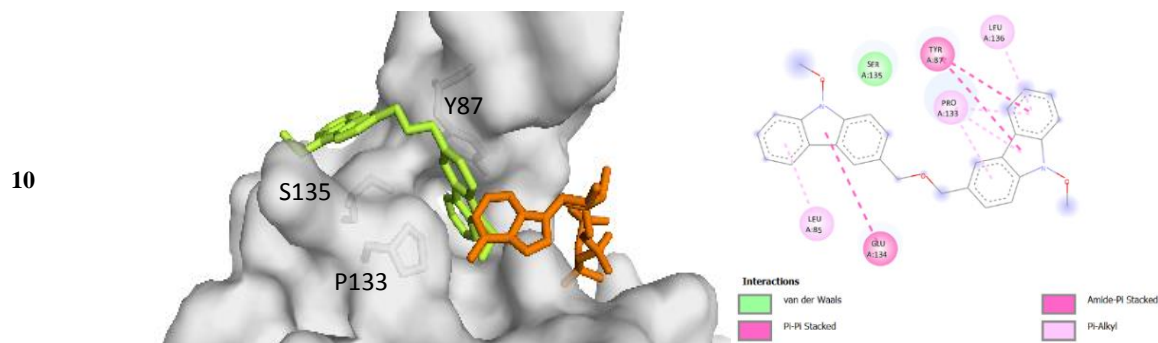
Compound 9 exhibited the highest number of interactions, forming nine alkyl and pi-alkyl interactions with essential amino acids. In contrast, compound 4 displayed only one pi-alkyl interaction with Pro133,

indicating that interaction quantity may influence binding affinity. Notably, compound 9 had a binding affinity (ΔG) of -7.2 kcal/mol, slightly lower than the -7.4 kcal/mol affinity exhibited by compound 4.

Table 3. The comparison of binding poses between PfAP4AH ligand candidates and ATP from molecular docking

No.	Comparison of ligand and ATP binding poses* and their 2D interactions with surrounding residues
1	
2	
3	
4	





*PfAp4AH ligand candidates are shown as green sticks, ATP as orange sticks, and residues Tyr87, Pro133, and Ser135 as grey sticks. The PfAp4AH protein is shown as a surface representation.

Compound 6 (bikoeniquinone A) interacted effectively with Tyr87, Pro133, and Ser135, forming hydrogen bonds (Ser135), an unfavorable interaction (Asn88), pi-pi stacking (Tyr87), and pi-alkyl bonding (Pro133). Despite the unfavorable interaction, compound 6 maintained a favorable ΔG of -7.3 kcal/mol, slightly lower than the highest observed affinity ($\Delta G = -8$ kcal/mol). Similarly, compound 10 showed analogous interactions but with a slightly lower affinity ($\Delta G = -7$ kcal/mol). These findings suggest that the type and quality of interactions are potentially more critical than their quantity in determining ligand binding affinity and overall stability within the receptor complex.

Carbazole alkaloids from *M. koenigii* emerged as highly promising PfAp4AH inhibitors, demonstrating binding affinities superior to ATP and establishing favorable interactions with critical active site residues. Notably, compound 1 exhibited robust inhibitory potential due to its diverse and strong interactions with key residues such as Tyr87, His43, Pro133, and Leu136. Although compound 9 had a higher number of interactions overall, its slightly lower binding affinity indicated that the quality and specificity of interactions are more influential than merely their quantity in determining binding affinity and therapeutic effectiveness.

Chemical structure analysis and a review of existing literature categorized these selected compounds as carbazole alkaloids or carbazole-derived alkaloids. Specifically, compound 1 was identified as a dimeric carbazole alkaloid derivative containing two carbazole units, structurally similar to known compounds from *M. koenigii* (Uvarani et al., 2013). Compound 2 (bismurrayaquinone A) was confirmed as a structurally characterized dimeric carbazole alkaloid derivative isolated from *M. koenigii* (Uvarani et al., 2013). Compound 3

(yuehchukene) is recognized as a dimeric indole alkaloid from related *Murraya* species (Kong et al., 1985). Compound 4 contains a distinct pyrano[3,2-a]carbazole structure, categorizing it clearly as a dimeric carbazole alkaloid (Uvarani et al., 2013).

Compound 5 (chrestifoline A) is typically classified as a carbazole alkaloid derivative isolated from *Murraya euchrestifolia* (Ito et al., 2006). Compound 6 (bikoeniquinone A) shares structural similarities with bismurrayaquinone, identifying it as a dimeric carbazole-derived quinone alkaloid (Uvarani et al., 2013). Compound 7 (8,8'-biskoenigine) is explicitly confirmed as a dimeric carbazole alkaloid derived from *M. koenigii* (Patel et al., 2016b). Compounds 8 and 9, structurally similar to compound 4, are categorized as pyrano-carbazole derivatives (Uvarani et al., 2013). Compound 10, characterized by carbazole units linked via an oxybis(methylene) bridge, is clearly confirmed as a carbazole alkaloid derivative.

4. Conclusion

This study identified Pocket 1 (P1) of PfAp4AH as a highly druggable and selective docking site, distinguished by unique residues not found in human homologs. Virtual screening and docking validation confirmed the reliability of the protocol and revealed ten carbazole alkaloids from *M. koenigii* with strong inhibitory potential, surpassing ATP in binding affinity. Notably, compound 1 demonstrated the most favorable and stable interactions with key active site residues, highlighting it as a promising lead. This is the first study to report *M. koenigii*-derived carbazole alkaloids as selective PfAp4AH inhibitors, offering a novel direction for antimalarial drug development.

References

- Ali, F., Wali, H., Jan, S., Zia, A., Aslam, M., Ahmad, I., Afridi, S. G., Shams, S., & Khan, A. (2021). Analysing the essential proteins set of *Plasmodium falciparum* PF3D7 for novel drug targets identification against malaria. *Malaria Journal*, 20(1), 335. <https://doi.org/10.1186/s12936-021-03865-1>
- Ashkenazy, H., Abadi, S., Martz, E., Chay, O., Mayrose, I., Pupko, T., & Ben-Tal, N. (2016). ConSurf 2016: An improved methodology to

estimate and visualize evolutionary conservation in macromolecules. *Nucleic Acids Research*, 44(W1), W344-W350. <https://doi.org/10.1093/nar/gkw408>

Ashley, E. A., Phyto, A. P., & Woodrow, C. J. (2018). Malaria. *The Lancet*, 391(10130), 1608-1621. [https://doi.org/10.1016/S0140-6736\(18\)30324-6](https://doi.org/10.1016/S0140-6736(18)30324-6)

Franyoto, Y. D., Nurrochmad, A., & Fakhrudin, N. (2024). *Murraya*

- koenigii* L. Spreng.: An updated review of chemical composition, pharmacological effects, and toxicity studies. *Journal of Applied Pharmaceutical Science*.
<https://doi.org/10.7324/JAPS.2024.169254>
- Ishikura, M., Imaizumi, K., & Katagiri, N. (2000). A concise preparation of yuehchukene and its analogues (Vol. 53).
- Ito, C., Itoigawa, M., Nakao, K., Murata, T., Tsuboi, M., Kaneda, N., & Furukawa, H. (2006). Induction of apoptosis by carbazole alkaloids isolated from *Murraya koenigii*. *Phytomedicine*, 13(5), 359-365. <https://doi.org/10.1016/j.phymed.2005.03.010>
- Jeyakanthan, J., Kanaujia, S. P., Nishida, Y., Nakagawa, N., Praveen, S., Shinkai, A., Kuramitsu, S., Yokoyama, S., & Sekar, K. (2010). Free and ATP-bound structures of Ap4A hydrolase from *Aquifex aeolicus* V5. *Acta Crystallographica Section D: Biological Crystallography*, 66(2), 116-124. <https://doi.org/10.1107/S0907444909047064>
- Kong, Y.-C., Cheng, K.-F., Cambie, R. C., & Waterman, P. G. (1985). Yuehchukene: A novel indole alkaloid with anti-implantation activity. *Journal of the Chemical Society, Chemical Communications*, (2), 47. <https://doi.org/10.1039/c39850000047>
- Patel, O. P. S., Mishra, A., Maurya, R., Saini, D., Pandey, J., Taneja, I., Raju, K. S. R., Kanojiya, S., Shukla, S. K., Srivastava, M. N., Wahajuddin, Tamrakar, A. K., Srivastava, A. K., & Yadav, P. P. (2016a). Naturally occurring carbazole alkaloids from *Murraya koenigii* as potential antidiabetic agents. *Journal of Natural Products*, 79(5), 1276-1284. <https://doi.org/10.1021/acs.jnatprod.5b00883>
- Patel, O. P. S., Mishra, A., Maurya, R., Saini, D., Pandey, J., Taneja, I., Raju, K. S. R., Kanojiya, S., Shukla, S. K., Srivastava, M. N., Wahajuddin, Tamrakar, A. K., Srivastava, A. K., & Yadav, P. P. (2016b). Naturally occurring carbazole alkaloids from *Murraya koenigii* as potential antidiabetic agents. *Journal of Natural Products*, 79(5), 1276-1284. <https://doi.org/10.1021/acs.jnatprod.5b00883>
- Saglam, M. F. (2022). Synthesis, characterization and thermal analysis of novel methylene bridged bis-carbazole based bisbenzimidazoles. *Hittite Journal of Science and Engineering*, 9(4), 281-286. <https://doi.org/10.17350/HJSE19030000281>
- Setyawati, I., Setiawan, A. G., Nemchinova, M., & Vidilaseris, K. (2024). The potential inhibitory mechanism of EGCG against the chikungunya virus targeting non-structural protein 2 through molecular dynamics simulation. *Scientific Reports*, 14(1), 29797. <https://doi.org/10.1038/s41598-024-81287-0>
- Sharma, A., Yogavel, M., & Sharma, A. (2016a). Structural and functional attributes of malaria parasite diadenosine tetraphosphate hydrolase. *Scientific Reports*, 6(1), 19981. <https://doi.org/10.1038/srep19981>
- Sharma, A., Yogavel, M., & Sharma, A. (2016b). Structural and functional attributes of malaria parasite diadenosine tetraphosphate hydrolase. *Scientific Reports*, 6(1), 19981. <https://doi.org/10.1038/srep19981>
- Uvarani, C., Sankaran, M., Jaivel, N., Chandraprakash, K., Ata, A., & Mohan, P. S. (2013). Bioactive dimeric carbazole alkaloids from *Murraya koenigii*. *Journal of Natural Products*, 76(6), 993-1000. <https://doi.org/10.1021/np300464t>
- White, N. J., Pukrittayakamee, S., Hien, T. T., Faiz, M. A., Mokuolu, O. A., & Dondorp, A. M. (2014). Malaria. *The Lancet*, 383(9918), 723-735. [https://doi.org/10.1016/S0140-6736\(13\)60024-0](https://doi.org/10.1016/S0140-6736(13)60024-0)
- World Health Organization (WHO). (2022). *World malaria report 2022*.